JOURNAL OF MATERIALS SCIENCE 28 (1993) 251–258

Preparation, and structural, optical and electrical properties of the $CdTe_{1-x}S_x$ system

S. K. J. AL-ANI, M. N. MAKADSI, I. K. AL-SHAKARCHI
Department of Physics, College of Science, University of Baghdad, Jadirya, Baghdad, Iraq
C. A. HOGARTH
Department of Physics, Brunel University, Uxbridge, Middlesex UB8 3PH, UK

Thin films of the $CdTe_{1-x}S_x$ system ($0<x<1$) have been prepared by a thermal evaporation technique, and their structural, optical and electrical properties have been measured in order to characterize the system. Detailed X-ray analysis showed that the structures are polycrystalline and the interplanar distances have been calculated for those systems. The $CdTe_{0.4}S_{0.6}$ system showed a maximum optical absorption. It is observed that the optical gap, E_{opt}, is indirect for ($0<x<0.5$) while for ($0.6<x<1$) it is direct. The variation of E_{opt} with x in the $CdTe_{1-x}S_x$ system is not linear and the minimum value of E_{opt} was for $x=0.3$. The addition of copper dopants up to 3% to the $CdTe_{0.4}S_{0.6}$ system reduced the value of E_{opt}. The electrical conductivity showed two values of activation energy indicating different dominant conduction mechanisms in different temperature ranges.

1. Introduction

The II–VI compound materials are the oldest that have been used on an industrial scale for the production of semiconductors and related devices [1]. They are used as cathode-ray tube screen materials, electroluminescent devices, ultraviolet responsive pigments, flash detectors and even as photoconductors and solar cells [2, 3]. During recent years the development of thin-film solar cells for terrestrial use has been documented because solar energy is an attractive energy alternative. Some efforts have been devoted to producing graded layer systems from two compounds differing in their energy gap. Indeed semiconductor alloys have been used for years to tune band gaps and average bond lengths to specific applications. By changing the concentrations and under controlled preparation conditions, it is possible to produce graded layers having a series of different values of energy gap, thus enhancing the absorption of the wavelengths incident on this film. Systems such as $Zn_xCd_{1-x}S$ [4], $CdTe_{1-x}S_x$ and ZnS_xTe_{1-x} [5–8] have been investigated. Radojcic *et al.* [9] have further suggested that mixed or graded thin-film devices such as solar cells, for example, based on CdS and CdTe semiconductors may overcome the limitation of using the two individual materials, by reducing the manufacturing costs and fabricating high-efficiency graded band gap $CdTe_{1-x}S_x$ thin film solar cells.

In the present work the preparation techniques as well as the structural, electrical and optical properties of the $CdTe_{1-x}S_x$ system have been investigated for different x values ($0 \leq x \leq 1$), and the optimum value for maximum solar absorption has been established.

2. Experimental procedure

2.1. Sample preparation

Thin films of CdS and CdTe were prepared by thermal evaporation from a covered molybdenum boat in a Balzers BAL 370 coating unit with ultimate pressure $\sim 1\times10^{-7}$ torr (1 torr = 133.322 Pa) rising to 1×10^{-6} torr during the evaporation process. The chamber and its components were initially cleaned with pure ethanol followed by dry nitrogen gas in a glow discharge. For aluminium electrode coating, an Edwards E 12 System with a vacuum $\sim 1.5\times10^{-5}$ torr was used. Soda–lime slides were used as substrates and were cleaned conventionally [10]. Different film geometries were achieved by the use of different mask shapes. Film thicknesses were determined during evaporation by the use of the quartz crystal monitor technique. This was complemented by a multiple beam interferometric method outside the vacuum. Growth rate was about $0.8\ nm\ s^{-1}$. The values of x have been taken in steps 0.1, 0.2, . . ., 1.0.

2.2. Measurements

The weight percentages that constituted the different compositions were pre-determined, and put together in a molybdenum boat prior to evaporation. Films were formed by condensation on substrates kept at room temperature. X-ray diffractometry was used to ascertain the crystal structure of all $CdTe_{1-x}S_x$ compositions, and for calculating the lattice constants for the crystal forms.

The electrical conductivity of the samples was obtained at different temperatures by measuring the current through the sample and a series resistor using a Keithley 616 electrometer. The temperatures were determined with a thermocouple. The temperature range was from room temperature to 523 K.

The optical absorption measurements were made at room temperature using a Pye-Unicam PV 8800 UV–visible spectrophotometer. The optical absorption coefficient, $\alpha(\omega)$, as function of the angular frequency of radiation, ω, was calculated from the measured optical absorbance, A, using the relation [11]

$$\alpha(\omega) = 2.303 \frac{A}{t} \quad (1)$$

where t is the actual film thickness.

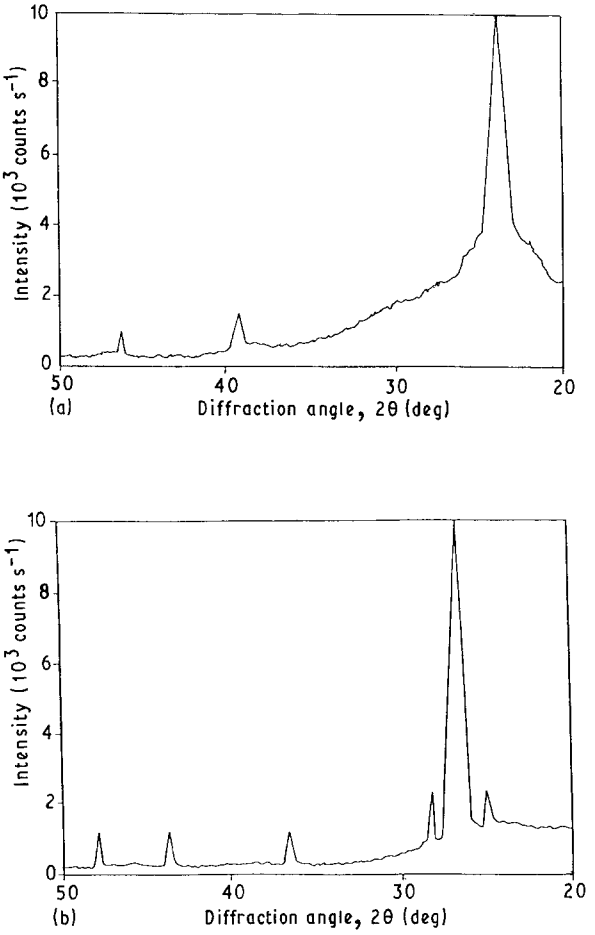

Figure 1 X-ray diffraction pattern of (a) CdTe and (b) CdS films annealed at 443 K.

3. Results and discussion

3.1. Structural study

Figs 1 and 2 show the X-ray diffraction patterns of CdTe, CdS and $CdTe_{1-x}S_x$ thin films before and after annealing at $T = 443$ K for about 30 min. They are of polycrystalline structure and from them we have calculated the interplanar distances, d. These distances, however, vary with the displacement of the Bragg angles for all $CdTe_{1-x}S_x$ systems and according to the ASTM index and Fig. 1, it is found that CdTe has a cubic unit cell (zinc blende) while CdS is of a würtzite unit cell [12, 13]. For the $CdTe_{1-x}S_x$ system, on the other hand, no ASTM information is available and therefore we have relied on the spectral analysis of the X-ray diffractometer in finding the Bragg angles. It has been observed that this angle is displaced towards CdS angles as the value of x in the system is increased. It has also been noted that a change in the structures between the zinc blende and würtzite occurs at $x \geq 0.5$ which confirms what has earlier been pointed out by Ohata *et al.* [7, 8] but they claimed the change is at $x = 0.2$, while in our work the change to the würtzite structure was for $x \geq 0.5$ which is more legitimate. Annealing up to $T = 443$ K did not change the maxima of Bragg peaks for all compositions ($0 \leq x \leq 1$) under examination, and this is because annealed films of low thickness ($t \sim 200$ nm) do not increase the growth of the grains. Instead they are attached together. This, in fact, explains the lack of change of Bragg peaks for all the $CdTe_{1-x}S_x$ system. Table I details the information obtained for the $CdTe_{1-x}S_x$

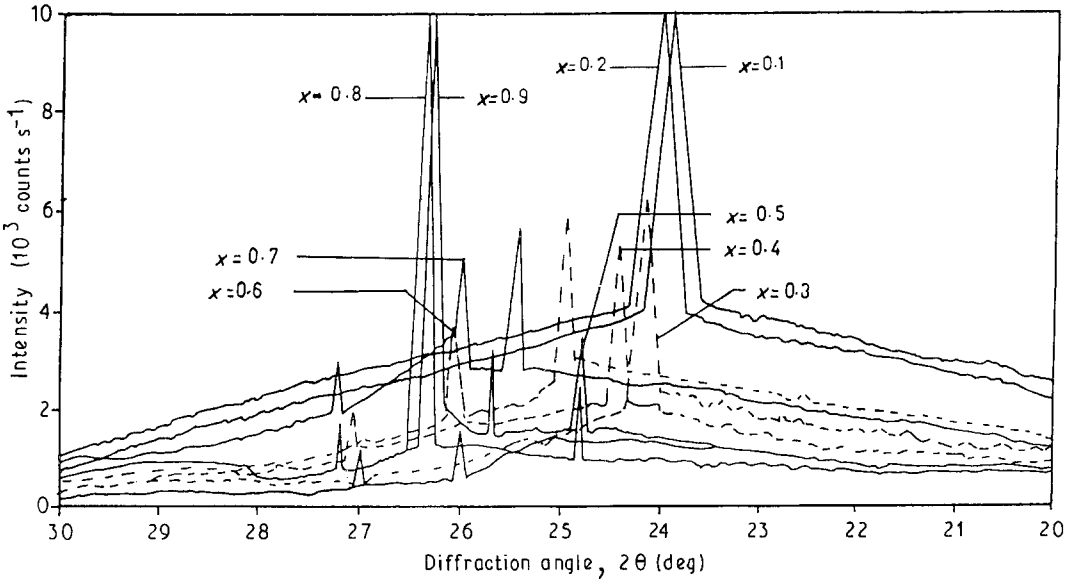

Figure 2 X-ray diffraction patterns of the $CdTe_{1-x}S_x$ system where $0.1 \leq x \leq 0.9$ before and after annealing at 443 K.

TABLE I The constants of the $CdTe_{1-x}S_x$ system from X-ray diffraction patterns

x	2θ (deg)	d (nm)	$h\,k\,l$		a (nm)	c (nm)
0	23.7	0.375	1 1 1	Zinc blende	0.6496	
	39.1	0.2301	2 2 0	Zinc blende		
	45.95	0.1973	3 1 1	Zinc blende		
0.1	23.9	0.3719	1 1 1	Zinc blende	0.6443	
	39.2	0.2296	2 2 0	Zinc blende		
	46.3	0.1947	3 1 1	Zinc blende		
0.2	24	0.3704	1 1 1	Zinc blende	0.6416	
	39.25	0.2293	2 2 0	Zinc blende		
	46.45	0.1953	3 1 1	Zinc blende		
0.3	24.15	0.3682	1 1 1	Zinc blende	0.6377	
	40	0.2252	2 2 0	Zinc blende		
	45.65	0.1985	3 1 1	Zinc blende		
0.4	24.4	0.3644	1 1 1	–	0.6311	
	40.3	0.2235	2 2 0	Zinc blende		
	47	0.1931	3 1 1	Zinc blende		
0.5	24.8	0.3586	1 0 0	Würtzite	0.3586	
	26	0.3424	0 0 2	Würtzite		0.6848
	27.1	0.3287	1 0 1	Würtzite		
	35.1	0.2554	1 0 2			
	40.35	0.2233	1 1 0			
	45	0.2012	1 0 3			
0.6	24.9	0.3572	1 0 0	Würtzite	0.3572	
	26.05	0.3417	0 0 2			0.6834
	27.05	0.3293	1 0 1	Würtzite		
	36.2	0.2479	1 0 2	Würtzite		
	42	0.2149	1 1 0	Würtzite		
	45.5	0.2991	1 0 3	Würtzite		
0.7	25.4	0.3503	1 0 0	Würtzite	0.3503	
	26	0.3424	0 0 2	Würtzite		0.6758
	27.2	0.3275	1 0 1	Würtzite		
	36.1	0.2485	1 0 2			
	43	0.2101	1 1 0	Würtzite		
	46	0.1971	1 0 3	Würtzite		
0.8	24.8	0.3586	1 0 0	Würtzite	0.3586	
	26.35	0.3379	0 0 2	Würtzite		0.6758
	27.2	0.3275	1 0 1	Würtzite		
	36	0.2492	1 0 2	Würtzite		
	43.9	0.206	1 1 0	Würtzite		
	47	0.1931	1 0 3	Würtzite		
0.9	25.7	0.3463	1 0 0	Würtzite	0.3463	
	26.3	0.3385	0 0 2	Würtzite		0.677
	27.2	0.3275	1 0 1	Würtzite		
	36.25	0.2475	1 0 2	Würtzite		
	43.45	0.208	1 1 0	Würtzite		
	47.9	0.1897	1 0 3	Würtzite		
1.0	24.8	0.3586	1 0 0	Würtzite	0.3586	
	26.5	0.336	0 0 2	Würtzite		0.6721
	27.9	0.3195	1 0 1	Würtzite		
	36.65	0.2449	1 0 2	Würtzite		
	43.5	0.2078	1 1 0	Würtzite		
	47.8	0.1901	1 0 3	Würtzite		

system from X-ray examination. Furthermore, the $CdTe_{1-x}S_x$ system has been doped with different percentages of copper atoms. The reason for this is to obtain a p-type semiconductor of this system by the substitutional doping of copper atoms instead of cadmium atoms. Fig. 3 shows that the intensity of the Bragg peaks increased systematically with increasing copper up to 1% Cu in the system and then reduced for 2%–3% Cu. It is believed that the high copper content leads to difficulties in obtaining a regular distribution of the copper atoms which hampers Bragg reflections and, in turn, reduces the intensity, as is evident from Fig. 3.

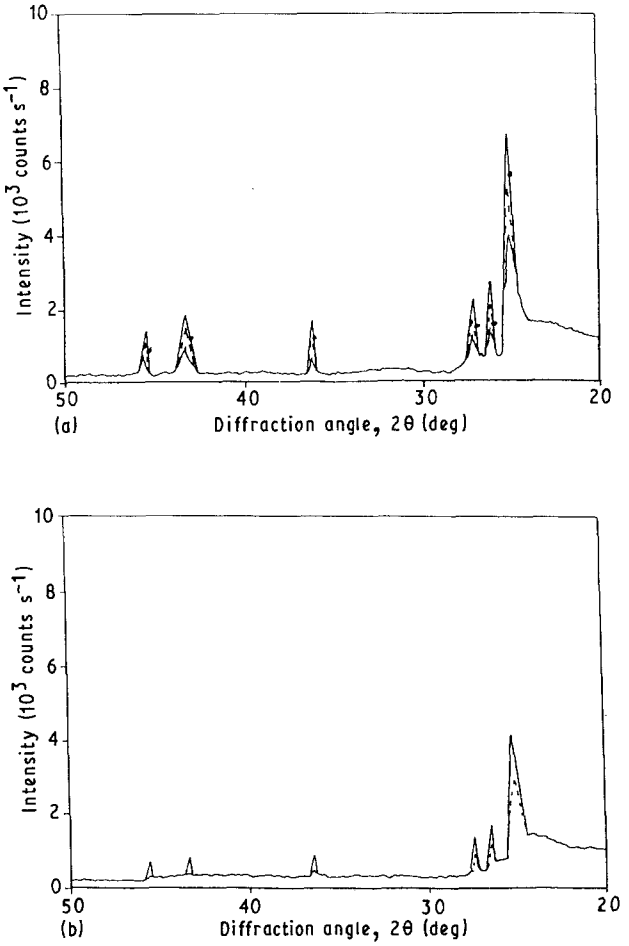

Figure 3 The X-ray diffraction pattern of a copper-doped $CdTe_{0.4}S_{0.6}$ film.

3.2. The electrical conductivity

Fig. 4 shows the change of conductivity, σ, versus x at room temperature for the $CdTe_{1-x}S_x$ system. Obviously the variation is not linear and σ changes steeply at nearly constant temperature when x approaches 0.5 from $2.77 \times 10^{-5}\,\Omega^{-1}\,cm^{-1}$ to $2.839\,\Omega^{-1}\,cm^{-1}$ for CdTe and CdS respectively. This is in fair agreement with previously published data [14–16]. It is clear from points of the graph [5] that it exhibits the conductivity of the films as-deposited and after annealing. The annealing process has reduced the conductivity for all compositions and this is due to the process of attachment of the granules, especially in low-dimensional films. The resistance of the areas separating those islands is quite high, giving rise to the reduction in conductivity after the first annealing. This is also supported by the X-ray result in the previous section, while during the increase of temperature from 303–443 K, log σ varies with inverse temperature which is a property known for semiconductors where the temperature coefficient of resistance is negative. The increase of σ with T is attributed to the growth of larger grain sizes which, in turn, increases the electron mean free path and reduces the scattering effect. The value of the activation energy, E_a, is obtained from the equation

$$\sigma = \sigma_0 \exp(-E_a/kT) \qquad (2)$$

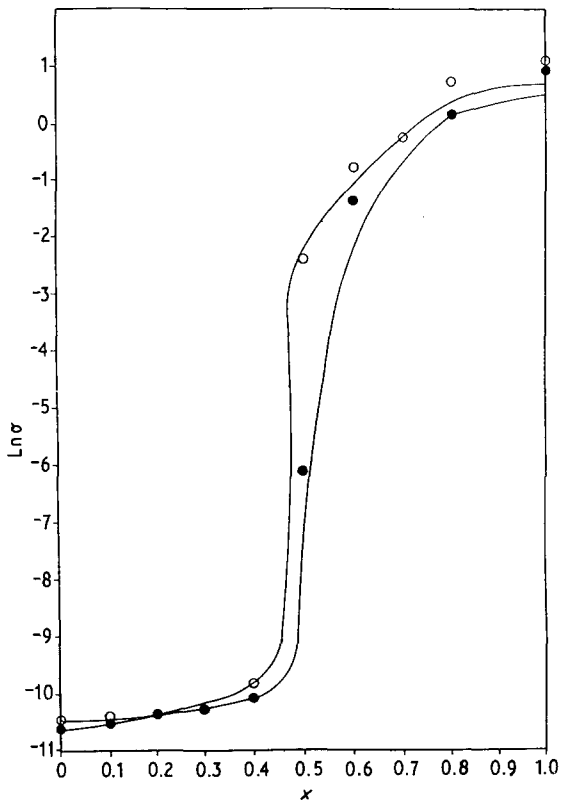

Figure 4 The variation of electrical conductivity with composition for the $CdTe_{1-x}S_x$ system (○) before and (●) after the first annealing process.

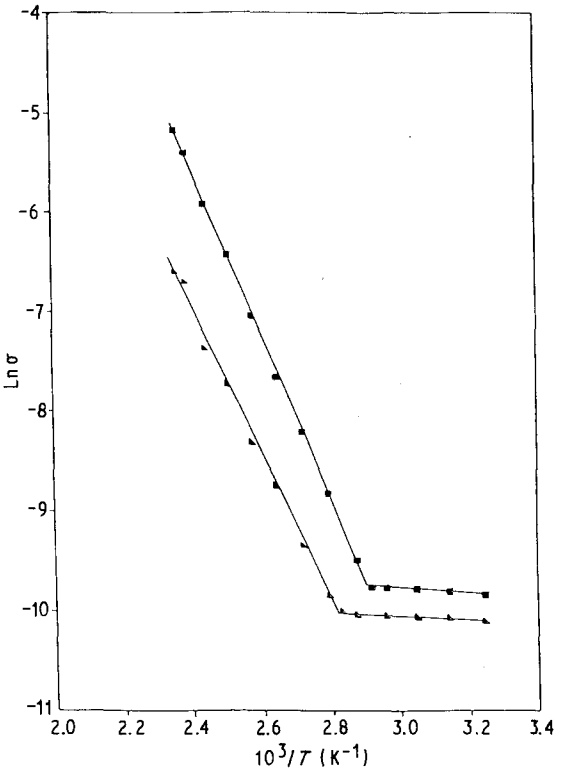

Figure 6 The variation of conductivity for the $CdTe_{1-x}S_x$ system with inverse temperature after the (■) first and (◣) second annealing processes.

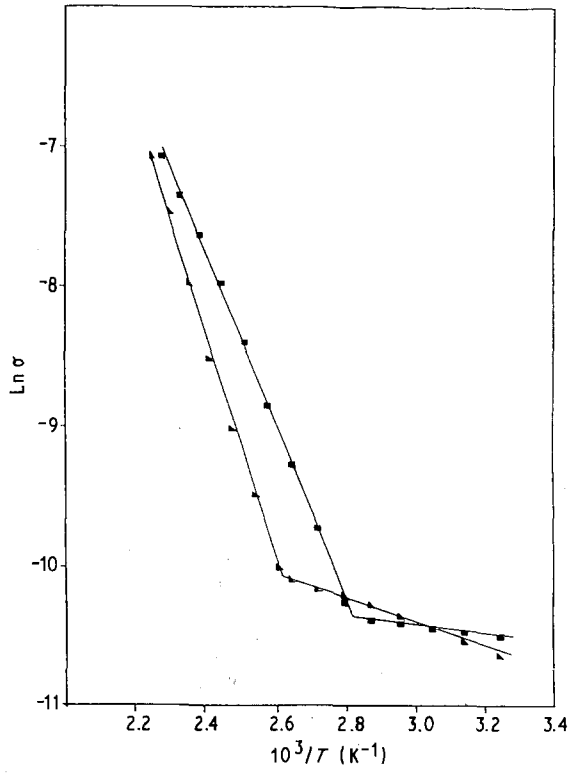

Figure 5 The variation of conductivity of a CdTe thin film with inverse temperature after the (■) first and (◣) second annealing processes ($x = 0$).

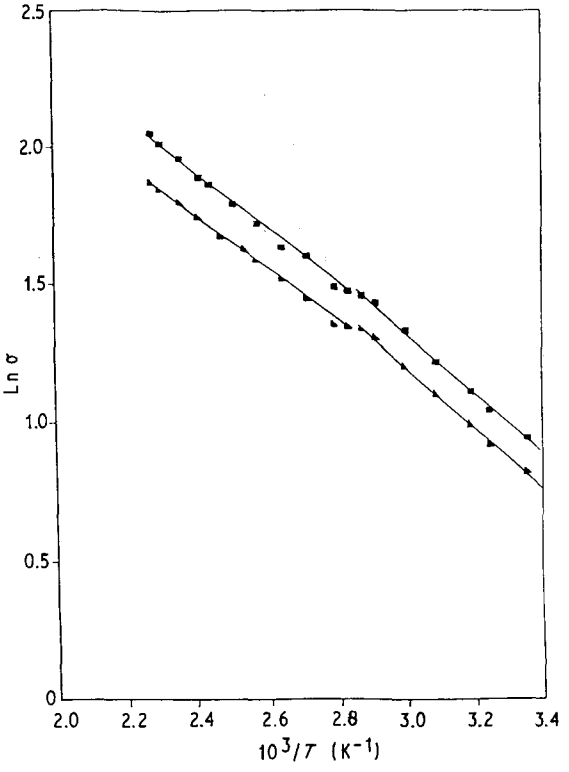

Figure 7 The variation of conductivity of a thin CdS film with inverse temperature after the (■) first and (◣) second annealing processes ($x = 1$).

where σ_0 is a constant and k is the Boltzmann constant. Figs 5–7 show a typical variation of ln σ versus $1000/T$ in accordance with Equation 2 for the CdTe, CdS and the $CdTe_{0.6}S_{0.4}$ systems. The values of E_a obtained for all $CdTe_{1-x}S_x$ systems after the first and second annealing processes are listed in Tables II and III, respectively. All the samples exhibit two linear regions i.e. two values of E_a. The first at the lower

TABLE II The values of activation energies in the temperature range studied for the $CdTe_{1-x}S_x$ system after the first annealing process

x	E_{a1} (eV)	Temperature range (K)	E_{a2} (eV)	Temperature range (K)	E_{a3} (eV)	Temperature range (K)
0	0.025	303–357	0.550	357–454		
0.1	0.243	327–370	0.427	384–444		
0.2	0.127	333–370	0.555	384–444		
0.3	0.452	333–392	0.702	400–434		
0.4	0.027	303–344	0.728	344–443		
0.5	0.255					
0.6	0.204	298–317	0.144	322–353	0.102	353–443
0.7	0.245	298–322	0.036	333–443		
0.8	0.168	298–357	0.076	357–443		
0.9	0.125	298–357	0.069	357–443		
1.0	0.102	298–344	0.184	357–443		

TABLE III The values of activation energies in the temperature range studied for the $CdTe_{1-x}S_x$ system after the second annealing process

x	E_{a1} (eV)	Temperature range (K)	E_{a2} (eV)	Temperature range (K)	E_{a3} (eV)	Temperature range (K)
0	0.077	303–377	0.709	384–454		
0.1	0.258	344–377	0.494	384–444		
0.2	0.126	333–370	0.479	389–444		
0.3	0.462	344–392	0.787	400–434		
0.4	0.024	303–348	0.661	357–443		
0.5	0.299	298–357	0.491	377–443		
0.6	0.230	298–338	0.171	338–384	0.131	384–443
0.7	0.322	298–322	0.070	333–443		
0.8	0.163	298–370	0.108	370–443		
0.9	0.158	298–357	0.166	370–443		
1.0	0.098	298–344	0.083	357–443		

temperatures is believed to be due to the transitions from the trapping levels in the band gap to the bottom of the conduction band or the top of the valence band, and the second is due to electron or hole transitions to conduction or valence bands, respectively. From Tables II and III, it is seen that in some films the value of E_{a2} is lower than E_{a1} (particularly for the $CdTe_{0.2}S_{0.8}$ system) and this is due to the re-arrangements of atoms at high temperature which leads to an increase in the scattering of conduction electrons where the vibrational range will be wider around its old or new positions at higher temperatures. It is also observed that the $CdTe_{0.4}S_{0.6}$ system exhibits a further slope E_{a3} in the high-temperature range, and this is attributed to electron transitions through the extended states in the conduction band. As we shall see later, $CdTe_{0.4}S_{0.6}$ has the highest optical absorbance which is essential for the present study, and thus this system will be considered in some detail.

Fig. 8 shows the variation of σ with different copper-doping levels. The lowest value obtained for conductivity occurred for the 0.25% Cu : $CdTe_{0.4}S_{0.6}$ system and starts to increase up to 3% Cu incorporation. Figs 9 and 10 show the variation of log σ versus inverse temperature for $CdTe_{0.4}S_{0.6}$ doped with different copper concentrations after the first and second annealing processes. Table IV summarizes the values of E_a obtained from Figs 9 and 10. It is seen that the disturbance in the curves of Fig. 9 for the doping levels 0.25%, 1% and 3% are smoothed out after the second annealing, as shown in Fig. 10. This may be because of a higher stability in the atomic arrangement. Two

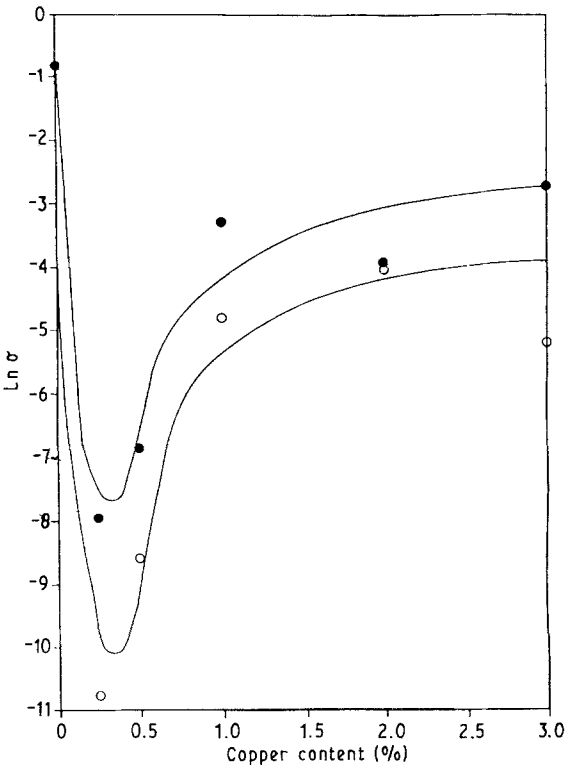

Figure 8 The variation of log conductivity with copper content for three samples of $CdTe_{0.4}S_{0.6}$ with different copper contents; (●) before annealing, (○) after annealing.

values of E_a are also observed (Table IV). These arise from the presence of several doping and trapping levels within the band gap and the dominance of each in a particular temperature interval. The exception

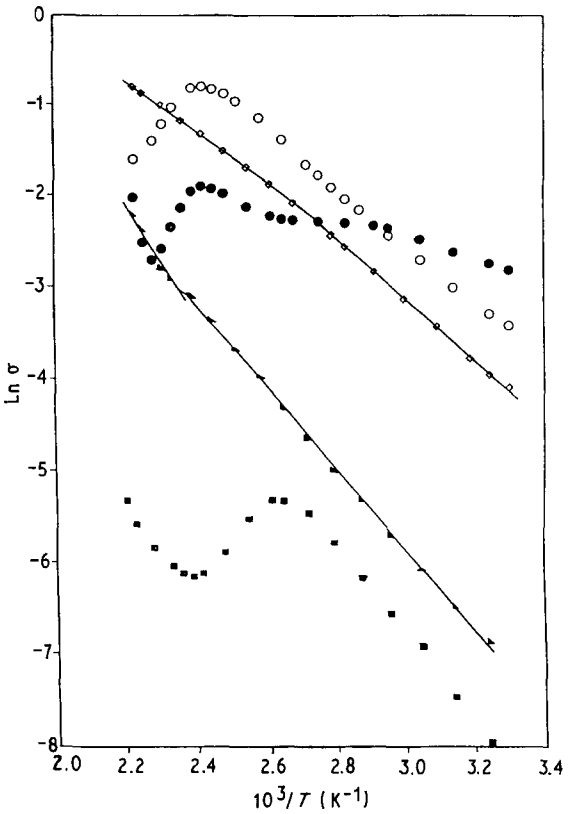

Figure 9 Variation of log conductivity with inverse temperature for the $CdTe_{0.4}S_{0.6}$ system doped with different copper contents after the first annealing. (■) 0.25% Cu, (◣) 0.5% Cu, (○) 1% Cu, (□) 2% Cu, (●) 3% Cu.

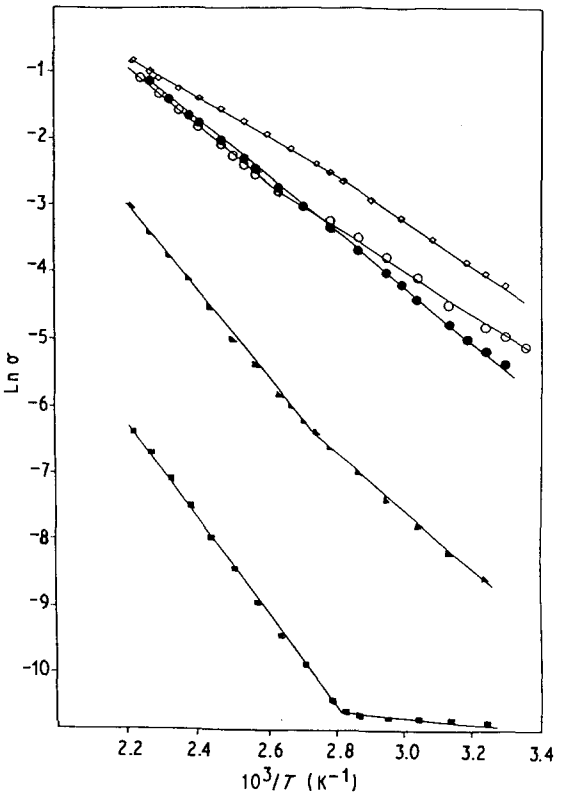

Figure 10 The variation of log conductivity with inverse temperature for the $CdTe_{0.4}S_{0.6}$ system doped with different copper contents after the second annealing. (■) 0.25% Cu, (◣) 0.5% Cu, (○) 1% Cu, (□) 2% Cu, (●) 3% Cu.

was 3% Cu which showed only one value of E_a. This may be due to incorporation of high copper content into the crystalline configuration and this view is also supported by the X-ray study.

3.3. The optical absorption

The optical absorbance of the $CdTe_{0.2}S_{0.8}$ system ($0 \leq x \leq 1$) in the wavelength range $\lambda \sim 300$–850 nm has been measured. Fig. 11 shows that the $CdTe_{0.4}S_{0.6}$ system has the highest optical absorption at $\lambda = 496$ nm. The optical band gap, E_{opt}, of the material has been obtained from the relation [17].

$$\alpha \hbar\omega \sim (\hbar\omega - E_{opt})^n \quad (3)$$

where $\hbar\omega$ is the energy of the incident photon and the exponent n may take values 1, 2, 3, $\frac{1}{2}$, $\frac{3}{2}$ depending on the electronic transitions in k-space. A linear fit was obtained for the $CdTe_{1-x}S_x$ system ($0 \leq x \leq 0.5$) with $n = 2$ (Equation 3), indicating indirect optical transitions were involved. A value of $E_{opt} \sim 1.56$ eV for $x = 0$ is obtained, which agrees well with other findings [9, 18]. For the $CdTe_{1-x}S_x$ system ($0.6 \leq x \leq 1$), the best fit was found using $n = \frac{1}{2}$ which

TABLE IV The values of E_a for the $CdTe_{0.4}S_{0.6}$ system doped with copper

Annealing process	Cu content (%)	E_{a1} (eV)	Temperature range (K)	E_{a2} (eV)	Temperature range (K)	E_{a3} (eV)	Temperature range (K)
1	0	0.204	298–317	0.144	322–353	0.102	353–443
	0.25						
	0.5	0.403	303–416	0.590	425–443		
	1.0						
	2.0	0.287	303–357	0.245	357–443		
	3.0						
2	0	0.230	298–338	0.171	338–384	0.131	384–443
	0.25	0.022	303–350	0.612	357–443		
	0.5	0.396	303–370	0.601	370–443		
	1.0	0.295	303–400	0.408	400–443		
	2.0	0.295	303–357	0.248	357–443		
	3.0	0.360	303–443				

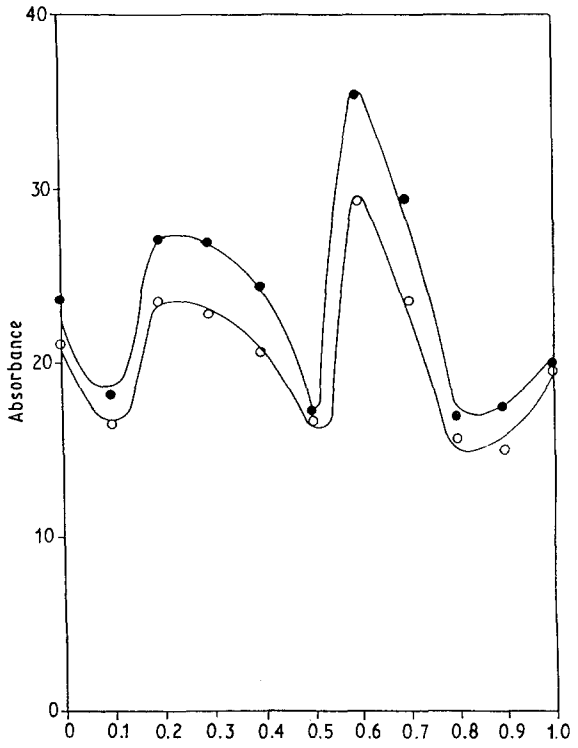

Figure 11 Variation of optical absorbance with x for a $CdTe_{1-x}S_x$ sample (●) before and (○) after annealing (λ = 496 nm).

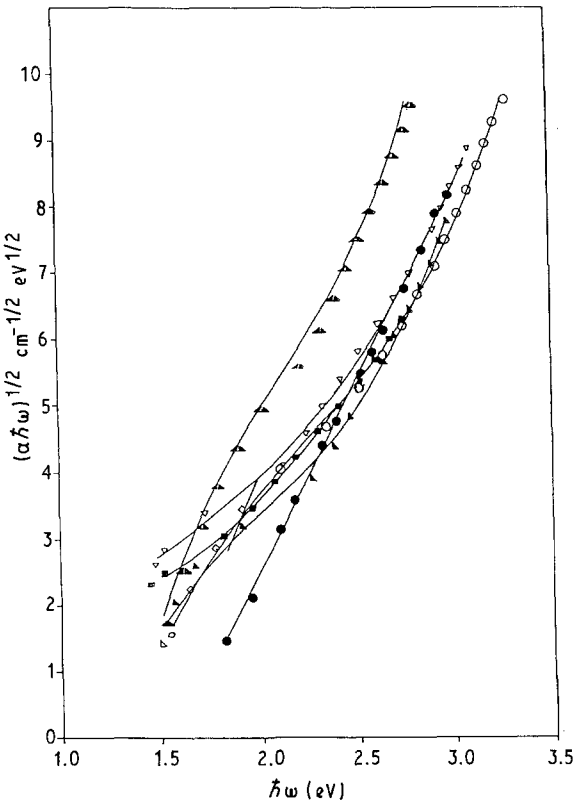

Figure 12 $(\alpha\hbar\omega)^{1/2}$ versus $\hbar\omega$ for the $CdTe_{1-x}S_x$ system before annealing (indirect transitions). E_g: (●) 1.56 eV, x = 0; (◣) 1.53 eV, x = 0.1; (◢◣) 1.40 eV, x = 0.2; (□) 1.29 eV, x = 0.3; (▽) 1.50 eV, x = 0.4 (○) 1.89 eV, x = 0.5.

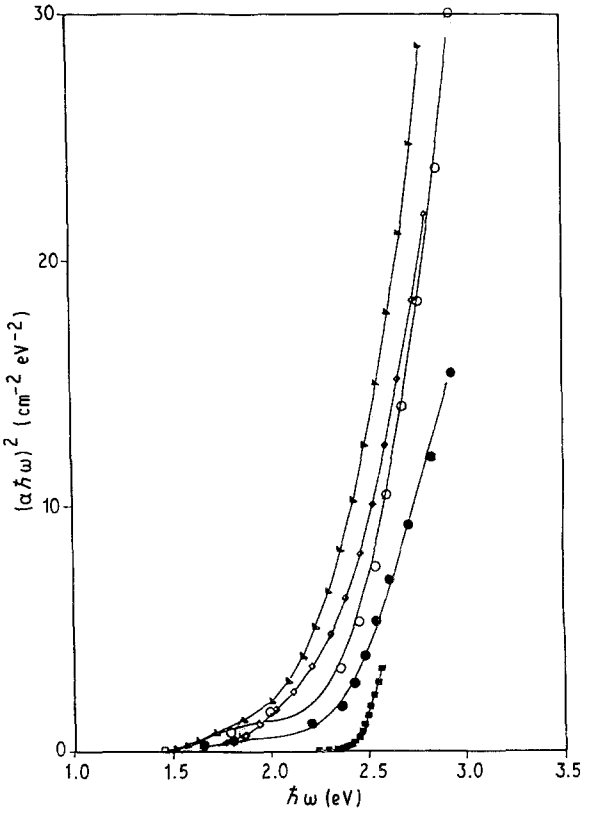

Figure 13 $(\alpha\hbar\omega)^{1/2}$ versus $\hbar\omega$ for the $CdTe_{1-x}S_x$ system before annealing (direct transitions). E_g: (◣) 2.24 eV, x = 0.6; (□) 2.28 eV, x = 0.7; (○) 22.36 eV, x = 0.8; (●) 2.39 eV, x = 0.9; (■) 2.34 eV, x = 1.0.

TABLE V (a) The variation of E_{opt} for the $CdTe_{1-x}S_x$ system with composition

x	E_{opt} (eV) (before annealing)	E_{opt} (eV) (after annealing)
0	1.56	1.76
0.1	1.53	1.68
0.2	1.40	1.47
0.3	1.29	1.35
0.4	1.50	1.77
0.5	1.89	2.00
0.6	2.24	2.66
0.7	2.28	2.58
0.8	2.36	2.56
0.9	2.39	2.68
1.0	2.43	2.63

(b) The variation of E_{opt} with copper content in the $CdTe_{0.4}S_{0.6}$ system

Cu content (%)	E_{opt} (eV) (before annealing)	E_{opt} (eV) (after annealing)
0	2.40	2.66
0.2	2.64	2.76
0.5	2.60	2.68
1.0	2.54	2.63
2.0	2.44	2.52
2.5	2.40	2.48

indicates that direct optical transitions were involved. For x = 1, however, the value of $E_{opt} \sim 2.43$ eV and this agrees with earlier work [19–21]. Figs 12 and 13 show the optical transitions in the $CdTe_{1-x}S_x$ system and Table V lists the values of E_{opt} before and after annealing. From this table, it is observed that for unannealed samples, the values of E_{opt} lie in the range 1.56–2.43 eV and vary non-linearly with the value of x.

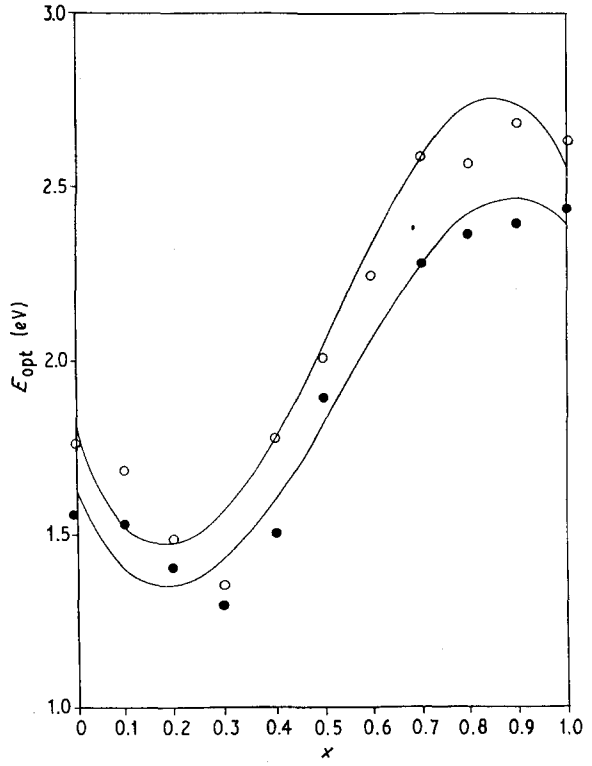

Figure 14 Variation of E_{opt} for a $CdTe_{1-x}S_x$ sample (●) before and (○) after annealing.

The lowest value was at $x = 0.3$ while Hill and Richardson [6] and Ohata *et al.* [7, 8] found it at $x = 0.2$ and 0.25, respectively. On annealing, E_{opt} has increased in general; the maximum E_{opt} within $0 \leq x \leq 1$, was 1.77 eV for $x = 0.5$. Fig. 14 exhibits the variation of E_{opt} with x for the $CdTe_{1-x}S_x$ system and fits the following equation

$$E_{opt}(x) = 1.62 - 3.14x + 10.361x^2 - 6.47x^3 \quad (4)$$

It is also seen from Table V that the value of E_{opt} has increased with annealing because the size of the crystallites has increased as well as the reduction of trapping levels inside the forbidden gap. The change in the optical transition from direct to indirect when changing the composition (i.e. x in the system) is also supported by X-ray examination as the structure has changed from zinc blende to würtzite at $x = 0.5$.

For the $CdTe_{0.4}S_{0.6}$ system doped with copper, the value of E_{opt} varied from 2.64–2.40 eV for 0.25% Cu and 3% Cu doping ratio, respectively. Table V represents the variation of E_{opt} with the copper doping ratio. From these results, one may conclude that on the addition of copper atoms, the doping levels will increase inside the band gap and the value of E_{opt} is thus reduced.

References

1. H. HARTMANN, R. MACH and S. SELLE, in "Current topics in materials science", Vol. **9** edited by E. Kaldis (North-Holland, Amsterdam, 1982) pp. 1–415.
2. D. B. HOLT, *Thin Solid Films* **24** (1974) 1.
3. T. M. RAZYKOV, *ibid.* **164** (1988) 301.
4. A. P. BELYAEV and I. P. KALINKIN, *ibid.* **158** (1988) 25.
5. R. HILL and D. RICHARDSON, *ibid.* **18** (1973) 25.
6. *Idem, J. Phys. C Solid State Phys.* **6** (1973) 1.
7. K. OHATA, J. SARALE and T. TANAKA, *Jpn J. Appl. Phys.* **12** (1973) 1641.
8. *Idem, ibid.* **12** (1973) 1198.
9. R. RADOJCIC, A. E. HILL and M. J. HAMPSHIRE, *Solar Cells* **4** (1981) 101.
10. I. K. AL-SHAKARCHI, MSc thesis, College of Science, Baghdad University (1989).
11. S. K. J. AL-ANI, C. A. HOGARTH and M. ILYAS, *J. Mater. Sci. Lett.* **3** (1984) 391.
12. P. SIKKA, K. V. FERDINAND, C. JUGADISH and P. C. MATHUR, *J. Mater. Sci.* **20** (1985) 246.
13. E. FATAS, P. HERRASTI, F. ARJONA, E. G. CAMARERO and M. LEON, *J. Mater. Sci. Lett.* **5** (1986) 583.
14. T. L. CHU, S. S. CHU, F. FIRSZT, H. A. NASEEM and R. STAWSKI, *J. Appl. Phys.* **58** (1985) 1349.
15. S. RAY, R. BANERJEE and A. K. BARUA, *Jpn J. Appl. Phys.* **19** (1980) 1889.
16. E. BERTRAN, J. L. MORENTA and J. ESTEVE, *Thin Solid Films* **123** (1985) 297.
17. L. L. KAZMERSKI (ed.), "Polycrystalline and amorphous thin films and devices" (Academic Press, London, 1980).
18. N. NAKAYAMA and H. MATSUMOTO, A. NAKANO, S. IKEGAMI, H. UDA and T. YAMASHITA, *Jpn J. Appl. Phys.* **19** (1980) 703.
19. I. MARTIL, G. G. DIAT and F. GUESADA, *Solar Energy Mater.* **12** (1985) 345.
20. T. M. RAZYKOV, *ibid.* **12** (1985) 233.
21. W. J. DANAHER, L. E. LYONS and G. C. MORRIS, *ibid.* **12** (1985) 137.

Received 23 March
and accepted 7 April 1992